

High-Resolution Angle Estimation for an Automotive FMCW Radar Sensor

Michael Schoor and Bin Yang
 Chair of System Theory and Signal Processing
 University of Stuttgart, Germany
 www.LSS.uni-stuttgart.de

Abstract—This paper introduces the application of high-resolution angle estimation algorithms for a 77GHz automotive long range radar sensor. High-resolution direction of arrival (DOA) estimation is important for future safety systems. Using FMCW principle, major challenges discussed in this paper are small number of snapshots, correlation of the signals, and antenna mismatches. Simulation results allow analysis of these effects and help designing the sensor. Road traffic measurements show superior DOA resolution and the feasibility of high-resolution angle estimation.

I. INTRODUCTION

In present automotive radar systems only targets in different range and velocity cells can be resolved. Increasing demand on safety functionality leads to efforts increasing the performance of angle estimation to allow resolution of targets in the same distance-velocity cell, for example two standing cars at the end of a traffic jam or other standing obstacles on the road. High-resolution methods for angle estimation such as MUSIC [1] or ESPRIT [2] enable radar sensors to resolve even very closely spaced targets. This is one important part of the KRAFAS project [3] (cost optimized radar sensor for active driver assistance systems) funded by the german ministry of education and research (BMBF). The goal of the project is to develop some low cost small sized 77GHz long-range radar (LRR) sensor capable of resolving two close targets with angle differences as low as 3 degrees [4].

Though the algorithms are well known in theory, major challenges must be met before application on real automotive FMCW radar systems. The major ones are discussed in this paper. It is organized as follows: Section II introduces the radar sensor concept and signal processing algorithms for FMCW radar systems as well as DOA estimation. Section III focuses on the application of high-resolution angle

estimation algorithms for automotive FMCW radar sensors. In section IV simulation results are shown as well as road traffic measurements showing the feasibility of high-resolution angle estimation algorithms with FMCW radar systems.

II. RADAR SENSOR CONCEPT AND SIGNAL PROCESSING

A. Frontend Concept

The specification of the automotive LRR sensor developed in the KRAFAS project includes a high estimation accuracy of $\theta_{\text{err}} \leq 0.4^\circ$ for the azimuth direction of arrival (DOA), an angular resolution of $\Delta\theta \leq 3^\circ$ and target ranges d up to 200m with relative target velocities v between $-60\frac{\text{m}}{\text{s}}$ and $20\frac{\text{m}}{\text{s}}$.

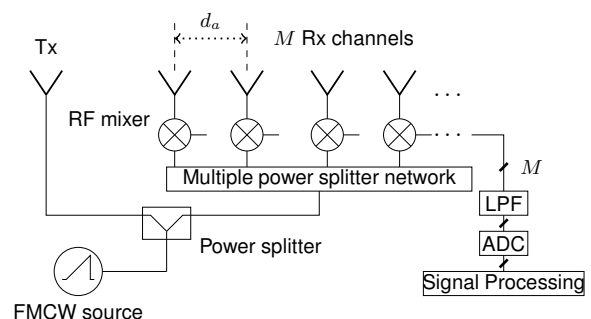


Fig. 1. Block diagram of the proposed FMCW radar frontend concept with M parallel Rx channels.

Fig. 1 shows a block diagram of the FMCW radar based frontend concept proposed in the KRAFAS project. The sensor basically is a bistatic radar sensor using M receive channels with identical distances d_a between each receive antenna, forming a so-called uniform linear array (ULA). This array allows using computationally efficient algorithms for DOA estimation such as Root-MUSIC [5] or ESPRIT, and also to use decorrelation algorithms such as forward backward averaging [6] and spatial smoothing [7].

B. FMCW Radar Signal Processing

Using a FMCW radar system, each target in a (d, v) cell corresponds to a baseband sinusoidal signal with a frequency depending on the ramp parameters such as slope and center frequency as well as target parameters d and v . Therefore the baseband signal is a mixture of multiple sinusoids. Using a FFT the baseband signals are transformed to frequency domain. Peak detection using CFAR principles for each ramp and matching leads to the target list containing distance and velocity of all detected targets. This can also be done in beamspace using digital beamforming (DBF), as better SNR and suppression of interferences from the side of the road improve performance. Finally the angles of all targets are estimated.

C. DOA Estimation

In the past conventional methods for DOA estimation such as amplitude matching (AM) [8] have been used in automotive radar systems. One important drawback of these methods is the lack of angular resolution due to the limited aperture size of the antenna, i.e. to resolve two or more closely spaced targets in the same (d, v) cell, which is important for future safety systems.

This is why high resolution methods are used to estimate the DOA of multiple targets. The angle resolution in this case is independent of the aperture size, under certain ideal assumptions like uncorrelated signals, high SNR, and long observations.

The family of subspace based high resolution methods uses an eigendecomposition of the (spatial) correlation matrix of the sensor signals to estimate the signal or noise subspace which is used for DOA estimation. The signal model for the received sensor signal \mathbf{x} is given by

$$\mathbf{x} = \mathbf{A}\mathbf{s} + \mathbf{n} \quad (1)$$

where $\mathbf{A} = [\mathbf{a}(\theta_1) \ \mathbf{a}(\theta_2) \ \dots \ \mathbf{a}(\theta_k)]$ is the steering matrix consisting of the steering vectors $\mathbf{a}(\theta) = [1, e^{j2\pi\frac{d}{\lambda}\sin(\theta)}, \dots, e^{j2(M-1)\pi\frac{d}{\lambda}\sin(\theta)}]^T$ of a uniform linear array, \mathbf{s} is the vector describing the k impinging signal waveforms and \mathbf{n} contains the sensor noise which is assumed to be spatially i.i.d. The correlation matrix and its eigendecomposition of \mathbf{x} is

$$\mathbf{R} = \mathbf{A}\mathbf{R}_s\mathbf{A}^H + \sigma^2\mathbf{I} = \mathbf{U}_s\mathbf{\Lambda}_s\mathbf{U}_s^H + \mathbf{U}_n\mathbf{\Lambda}_n\mathbf{U}_n^H \quad (2)$$

with the signal correlation matrix \mathbf{R}_s , the identity matrix \mathbf{I} , the signal subspace \mathbf{U}_s consisting of the k dominant eigenvectors, and the noise subspace \mathbf{U}_n consisting of the remaining $N - k$ eigenvectors. Since the column vectors of \mathbf{U}_s and \mathbf{A} span the same signal subspace, each peak in the MUSIC angular spectrum

$$w(\theta) = \frac{\mathbf{a}(\theta)^H \mathbf{a}(\theta)}{\mathbf{a}(\theta)^H \mathbf{U}_n \mathbf{U}_n^H \mathbf{a}(\theta)} \quad (3)$$

corresponds to a target DOA.

Other DOA estimators such as Root-MUSIC, ESPRIT or SUMWE [9] rely on the shifting property of the ULA. By dividing the array into several overlapping subarrays, their steering vectors for one target and several subarrays are identical. Obviously, these algorithms fail if this shifting property is violated, e.g. by imperfections of the antenna array.

One important step for subspace based high resolution methods is subspace estimation. This is done by computing an eigendecomposition of the spatial correlation matrix. Information theoretic criteria such as MDL or AIC can be used to estimate the number of signals [10]. If the subspace estimation fails, DOA estimators give wrong results such as high angle error, false or missed targets. There are several challenges to meet regarding subspace estimation, which will be explained in more details in the following sections.

D. Decorrelation

When signals are correlated, the condition of the signal correlation matrix \mathbf{R}_s is degraded and also the condition of the correlation matrix \mathbf{R} . This complicates subspace estimation and even leads to missed targets and high angle errors. Decorrelation algorithms help by reestablishing the condition of the signal correlation matrix. They make use of symmetry properties of the ULA. Forward backward averaging [6] uses the centrosymmetry property. The effective aperture is preserved, but the algorithm is limited to two correlated signals. Spatial smoothing [7] uses the shifting property. Subarrays are averaged and correlated signals up to the number of subarrays are possible. One drawback is that the effective aperture is reduced which limits accuracy of the estimated DOAs. Both algorithms, and also the combination of both, namely forward backward spatial smoothing (FBSS), rely on the symmetry properties. If these are violated e.g. by the forementioned imperfections of the antenna array, the estimated subspaces are disturbed and angle errors occur.

Window	$\Delta f = 1$ bin	2 bins	3 bins
Chebyshev 60dB	-5.9dB	-28.7dB	-62.6dB
Chebyshev 80dB	-4.4dB	-19.4dB	-59.1dB
Chebyshev 100dB	-3.5dB	-15.0dB	-38.5dB
Hamming	-7.4dB	-65.1dB	-73.6dB
Hann	-6.0dB	-63.7dB	-72.2dB

TABLE I
SIGNAL POWER LOSS OF FREQUENCY BINS ADJACENT TO A
PEAK BIN

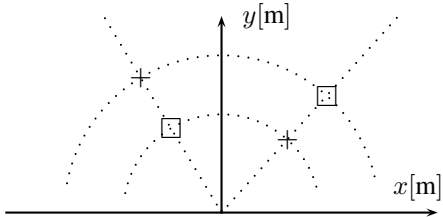


Fig. 2. “Butterfly targets” with frequency overlapping on FMCW radar systems. Real targets are marked with \square , false targets with $+$. Dotted lines represent constant angles or distances.

III. APPLICATION ON FMCW RADAR

A. FMCW: Number of snapshots and overlapping

A major challenge in the case of FMCW radar is the low number of snapshots. In frequency domain, only one to three bins can be used for angle estimation. Table I shows the theoretic signal power loss observed with different FFT windows when bins adjacent to the peak bin are used to estimate the correlation matrix. With a Chebyshev window (100dB sidelobe attenuation) the loss is only 3.5dB, therefore a high amount of signal energy is still contained in these bins. The number of snapshots can be increased, though they are not independent anymore. When using up to four FMCW ramps, the total number of snapshots can be as high as twelve.

Unfortunately, not all of these bins can be used. With the FMCW principle, several targets at different (d, v) cells can have the same baseband frequency. In this case, the corresponding samples contain the angle information of all involved targets. This can lead to false targets or “butterfly targets”. Fig. 2 illustrates an example for this situation: Given two real targets with different distances and relative velocities. They share the same frequency in one ramp. Using high-resolution angle estimation with all snapshots available for each (d, v) cell, two angles are detected, but only one is from the real target at the examined (d, v) cell. One way to solve this problem is to discard the affected FMCW ramp for angle detection, assuming that frequency overlapping can be detected.

B. Correlation of Signals

During measurements, it was often observed that signals were correlated. The degree of the correlation depends on the situation, but can be very high, close to coherence, for static scenarios. This could be considered as the worst case situation for high-resolution DOA estimation. It is hard to give an average correlation. Using decorrelation algorithms improves performance for correlated signals as well as for uncorrelated scenarios as smoothing virtually increases the number of snapshots.

C. Calibration mismatches

Most of the subspace based high-resolution DOA estimators rely on symmetry properties of the antenna array and knowledge of the RX channels. Due to various impairments of the RF frontend the complex baseband signal vector \mathbf{x}_s is a distorted version of the ideal received vector \mathbf{x}_r . The distortion can be modeled as

$$\mathbf{x}_s = \mathbf{G}\mathbf{P}\mathbf{C}\mathbf{x}_r \quad (4)$$

where \mathbf{G} and \mathbf{P} are diagonal matrices for gain and phase mismatches, respectively, and \mathbf{C} is a diagonally dominant matrix accounting for electromagnetic mutual coupling between the channels.

There are numerous methods for calibrating the received signal vector, i.e. searching for $(\mathbf{G}\mathbf{P}\mathbf{C})^{-1}$, e.g. [11], [12]. They are only capable of compensating global distortions, i.e. angle-independent errors. Angle-dependent gain and phase mismatches $\mathbf{G}(\theta)$ and $\mathbf{P}(\theta)$ are mainly due to antenna pattern inhomogeneities which occur e.g. due to finite size of the radome and radome reflections. Since each Rx element is positioned at a different lateral position behind the radome, the pattern distortions are different at each Rx channel.

In combination with correlated signals and decorrelation algorithms, this leads to limitations regarding angle resolution and accuracy. As the symmetry properties are no longer fulfilled, decorrelation algorithms disturb the subspace estimation which leads to angle errors. This effect is stronger, the higher the correlation of the signals and the higher the antenna imperfections are. While the second reason is quite obvious, the first one is because the decorrelation algorithms reestablish the condition of the signal correlation matrix. If the condition was already good because signals were uncorrelated, the erroneous contributions of the decorrelation algorithms are small.

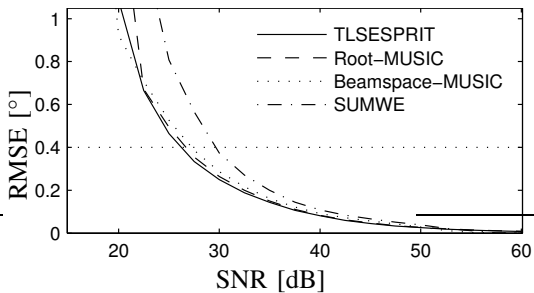


Fig. 3. RMSE vs. SNR for DOA estimation using one ramp, two coherent targets. All DOA except SUMWE use FBSS.

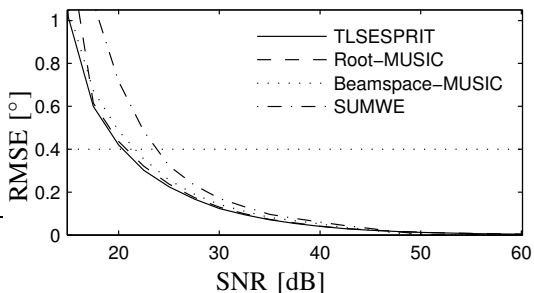


Fig. 4. RMSE vs. SNR for DOA estimation using four ramps, two coherent targets. All DOA estimators except SUMWE use FBSS.

IV. SIMULATION RESULTS AND MEASUREMENTS

A. Simulation of angular resolution

Simulations were performed to examine the resolution thresholds for DOA estimation using high-resolution algorithms. An ideal antenna array of $M = 8$ elements with $d_a = 1.0\lambda$ spacing was used in all simulations with FMCW ramps of 1ms length. As a worst case, two nearly coherent targets ($\rho = 0.9999$) in the same (d, v) cell were simulated with angles of $\theta_1 = -1.5^\circ$ and $\theta_2 = 1.5^\circ$ and equal SNR. Fig. 3 shows the RMSE of both targets for different DOA estimators using only one ramp for angle estimation with 1000 simulation runs. The desired angular accuracy of 0.4° is depicted as a dotted line. The required SNR is about 26–27dB for most estimators, and about 30dB for the SUMWE algorithm.

Fig. 4 shows the same scenario using four ramps for angle estimation. Now the algorithms need around 21–23dB and 24dB for SUMWE to meet the system specification.

Interestingly, subspace based high-resolution angle estimation is possible using just one single FMCW ramp, hence with three snapshots (frequency bins) which is smaller than the dimension of the correlation matrix. The number of targets was assumed to be

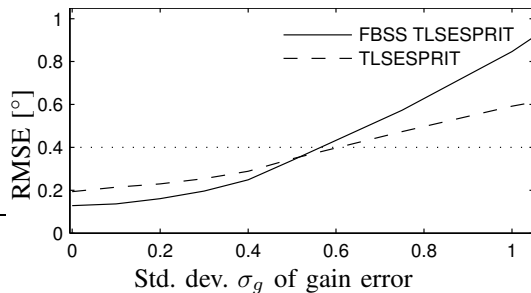


Fig. 5. RMSE vs. standard deviation σ_g of gain error for DOA estimation using four ramps, two uncorrelated targets.

known in all simulations. In practice the number of targets is unknown and has to be estimated in addition.

B. Simulation of mismatches

In all practical radar sensors, the antenna elements have different antenna patterns and other channel mismatches. Mismatches were simulated with log-normally distributed gain mismatches and the standard deviation σ_g . Two uncorrelated signals with equal SNR of 30dB were used in 10^5 runs. The RMSE is depicted for the TLS-ESPRIT DOA estimator, without and with FBSS. The results are depicted in Fig. 5.

For small gain mismatches, the FBSS TLS-ESPRIT algorithm gives better results as the smoothing performed prior to the eigenvalue decomposition increases virtually the number of snapshots and improves the subspace estimation. As the mismatches rise, more errors are introduced by the smoothing and angle errors rise above the results obtained without decorrelation. In our case, the intersection is around the specified angular accuracy, so using FBSS yields better results.

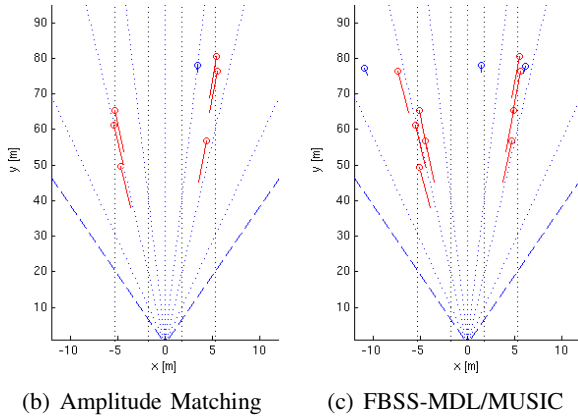
C. Measurements

Road traffic measurements were carried out in order to examine the feasibility of superresolution DOA estimation in practical application. The prototype radar sensor used an antenna array with $M = 16$ and $d_a = \lambda/2$ which gives the same aperture as in our simulations.

Fig. 6 shows a traffic scenario with a single car driving on the right lane. The road borders were equipped with metal guarding lanes, which are also very good radar reflectors. The DOA estimation results are shown in Fig. 6(b) for the AM algorithm



(a) Traffic scenario



(b) Amplitude Matching

(c) FBSS-MDL/MUSIC

Fig. 6. (a) Birdseye view of the traffic scenario, (b) DOA estimation using the AM algorithm (c) DOA estimation using the MDL/MUSIC algorithm combined with FBSS. Radial lines indicate relative velocity (doppler).

and in Fig. 6(c) for MDL algorithm for order estimation and MUSIC algorithm for DOA estimation, combined with FBSS. The target markers in the x-y-planes can be classified by the relative velocity. The car in front (low relative velocity) is clearly visible as well as reflections from guarding lanes (high relative velocity). The difference between (b) and (c) is that there is some major angle error in case of AM, estimating the car 2–3m further to the right, at the neighboring lane. This angle error can be assigned to the reflections from multipath propagation including the car and mirroring at the guarding lanes, being equivalent to some multi target scenario. This cannot be resolved in case of AM, but in case of MUSIC it is resolvable as can be seen in the figure.

V. SUMMARY

Some of the challenges when applying high-resolution DOA estimation for an automotive FMCW radar sensor were discussed. The major ones are the low number of snapshots, correlation of signals, and antenna mismatches. This requires the use of decorrelation algorithms which interferes with antenna mismatches. System simulations show which correlations and mismatches can be tolerated to meet the specified angular accuracy of 0.4° and the angular resolution of $\Delta\theta = 3^\circ$. Road traffic measurements

show the feasibility of high-resolution DOA estimation algorithms and the advantage of the new algorithms to standard amplitude matching.

ACKNOWLEDGMENT

The authors would like to acknowledge the funding of the German Ministry of Education and Research (BMBF) under contract nr. 16SV2181 (KRAFAS) and the cooperation of all partners of the KRAFAS consortium. They also would like to thank Robert Bosch GmbH for the support during the measurements.

REFERENCES

- [1] Ralph O. Schmidt, "Multiple emitter location and signal parameter estimation," *IEEE Trans. Antennas and Propagation*, vol. 34, no. 3, pp. 276–280, Mar. 1986.
- [2] Richard Roy and Thomas Kailath, "ESPRIT – Estimation of signal parameters via rotational invariance techniques," *IEEE Trans. Acoustics, Speech, and Signal Processing*, vol. 37, no. 7, pp. 984–995, July 1989.
- [3] Martin Schneider, "KRAFAS - Innovationen in der Mikrosystemtechnik und der Hochfrequenz-Mikroelektronik für kostenoptimierte Radarsensoren im Automotive-Bereich," in *VDE Kongress*, Aachen, 2006, pp. 275–282.
- [4] Peter Wenig, Michael Schoor, Oliver Günther, Bin Yang and Robert Weigel, "System design of a 77GHz automotive radar sensor with superresolution DOA estimation," in *Proc. Int. Symposium on Signals, Systems, and Electronics (ISSSE)*, July 2007.
- [5] Arthur J. Barabell, "Improving the resolution performance of eigenstructure-based direction finding algorithms," in *Proc. IEEE Conference on Acoustics, Speech, and Signal Processing (ICASSP)*, vol. 8, Apr. 1983, pp. 336–339.
- [6] Guanghan Xu and Thomas Kailath, "Detection of number of sources via exploitation of centro-symmetry property," *IEEE Trans. Signal Processing*, vol. 42, no. 1, pp. 102–112, Jan. 1994.
- [7] Tie Jun Shan, Mati Wax and Thomas Kailath, "On spatial smoothing for estimation of coherent signals," *IEEE Trans. Acoustics, Speech, and Signal Processing*, vol. 33, no. 4, pp. 806–811, Aug. 1985.
- [8] Merrill I. Skolnik, *Introduction to RADAR Systems*, 3rd ed. McGraw-Hill, 2001.
- [9] Jingmin Xin and Akira Sano, "Computationally efficient subspace-based method for direction-of-arrival estimation without eigendecomposition," *IEEE Transactions on Signal Processing*, vol. 52, no. 4, pp. 876–893, Apr. 2004.
- [10] Mati Wax and Thomas Kailath, "Detection of signals by information theoretic criteria," *IEEE Trans. Acoustics, Speech, and Signal Processing*, vol. 33, no. 2, pp. 387–392, Apr. 1985.
- [11] C. M. S. See, "Sensor array calibration in the presence of mutual coupling and unknown sensor gains and phases," *Electronics Letters*, vol. 30, no. 5, pp. 373–374, Mar. 1994.
- [12] J. Pierre and M. Kaveh, "Experimental performance of calibration and direction-finding algorithms," in *Proc. IEEE Conference on Acoustics, Speech, and Signal Processing (ICASSP)*, 1991.